Shape and Dimensions of Gel-Domains in Phospholipid Bilayers: A Theoretical Study

Vladimir Smorodin*,†,‡,§ and Eurico Melo†,||

Instituto de Tecnologia Química e Biológica, Oeiras, Portugal, Faculty of Chemistry, Moscow State University, Moscow, Russia, Center for Chemical Physics, University of Western Ontario, London, Canada, and Instituto Superior Técnico, Lisboa, Portugal

Received: November 30, 2000; In Final Form: March 21, 2001

It is now well established that in the gel-fluid phase coexisting region of bilayers made of two mixed phospholipids, one of the phases is microdispersed in the other. On the basis of data obtained with fluorescence recovery after photobleaching for 1,2-dimyristoyl-*sn*-glycero-(3)-phosphocholine/1,2-distearoyl-*sn*-glycero-(3)-phosphocholine (DMPC/DSPC) mixtures, the linear dimension of the rigid domains for small rigid phase fractions was predicted to be 2−3 μm (Coelho, F. P. ; Vaz, W. L. C.; Melo, E. *Biophys. J.* **1997**, *72*, 1501) and therefore, much smaller than the domains obtained with monolayers with identical composition. Recent "nanoscopic" observations confirmed that this was a reasonable estimate. In this work, we explain this difference in dimension, ascribing it to the interaction of the polarized surface of the two opposing domains pertaining to the two bilayer leaflets. It is shown that the geometry of the rigid structures formed is strongly dependent on the bilayer core dielectric permittivity. It is also found that in bilayers a circular to elliptic shape transition, similar to the one predicted for monolayers, is to be expected.

Introduction

In certain ranges of temperature and pressure, mixtures of lipids organized in monolayers or bilayers separate in immiscible phases, eventually one of them solidlike, so-called gel, and the other fluid.[1]

This phase separation has been observed in Langmuir−Blodgett monolayers made of pure or mixed lipids doped with fluorescent probes that partition almost exclusively into the fluid or less ordered phase.[2] Probes with this property are easy to design since it is known that a short chain phospholipid in a matrix of longer chain molecules or an unsaturated phospholipid in a mixture of saturated ones will dissolve preferentially in the disordered phase. The rigid domains that develop upon isothermal compression or isobaric cooling of fluid monolayers doped with these fluorescent probes are visible with an optical fluorescence microscope[2,3] and have been observed to grow in rodlike or spiral-like forms depending on the chirality of the lipids used, and on the presence or absence of cholesterol.[4]

In bilayers, however, it has not been possible to observe the coexisting phase domains or their geometry with conventional optical microscopy, presumably because in this case, at least one of the linear dimensions of the objects is submicroscopic (smaller than or of the order of magnitude of $\lambda/2$, the Abbé limit). Electron microscopy is not of much help in the study of such systems because the sample preparation procedure may disturb the equilibrium. Recent microscopic techniques with nanometer resolution, a resolution adequate for this type of sample, are still under development. However, some preliminary results obtained with near-field microscopy confirm that the lipid domains in deposited multilayers[5] and in cells[6] are of the order of a few μm. Confocal fluorescence correlation microscopy allowed Korlach et al.[7] the direct observation the process of domain formation in 1,2-dilauroyl-*sn*-glycero-(3)-phosphocholine/1,2-dimyristoyl-*sn*-glycero-(3)-phosphocholine mixtures. Their images confirm that for low rigid fractions the phase rich in the longest tail phospholipid forms structures of size of a few μm. However, Bagatolli and Gratton[8] show results that seem to contradict those previously referred. The dimensions of the domains are larger than 10 μm and a single domain is in general observed in giant unilamellar vesicles which do not allow for percolative diffusion as observed in several systems by other authors.[9]

The technique of fluorescence recovery after photobleaching, FRAP, has been the first to be used for the indirect observation of phase separation in mixed lipid bilayers.[9,10−13] In FRAP, we measure the rate of arrival to the central spot (the photobleached area) of tracer molecules that are considered exclusively soluble in the fluid phase, having on their way sampled the intricacies of the membrane topology, i.e., we observe the result of the two-dimensional molecular percolation through the system. Depending on the fraction of the rigid phase, a variety of behaviors is observed. For small solid fractions, the recovery of fluorescence is slower than what is to be expected for an equivalent fluid bilayer, due to the hindrance to diffusion caused by the dispersed solid domains. Above a certain solid fraction, depending on the mixture under study, only a partial recovery with a long tail is obtained. Such behavior is the consequence of the reservoir of tracer molecules accessible to the FRAP spot being finite. The rigid/fluid domains formed, and their topology, seem to correspond to a thermodynamically equilibrated state given that the FRAP results are independent of being obtained from a heating or cooling run, and the molecular percolation in the system is not modified after the system has been held for a long time at a stable temperature.

* To whom correspondence should be addressed. Vladimir Smorodin, CCP, Physics & Astronomy Department, University of Western Ontario, London, Ontario, N6A 3K7 Canada. Email: v_smorodin@hotmail.com. Phone: 1-519-661 2111, ext.86861. Fax: 1-519-661-3032.

† Instituto de Tecnologia Química e Biológica, Oeiras, Portugal.

‡ Faculty of Chemistry, Moscow State University, Moscow, Russia.

§ Center for Chemical Physics, University of Western Ontario, London, Canada.

|| Instituto Superior Técnico, Lisboa, Portugal.

10.1021/jp0043322 CCC: $20.00
Published on Web 06/05/2001

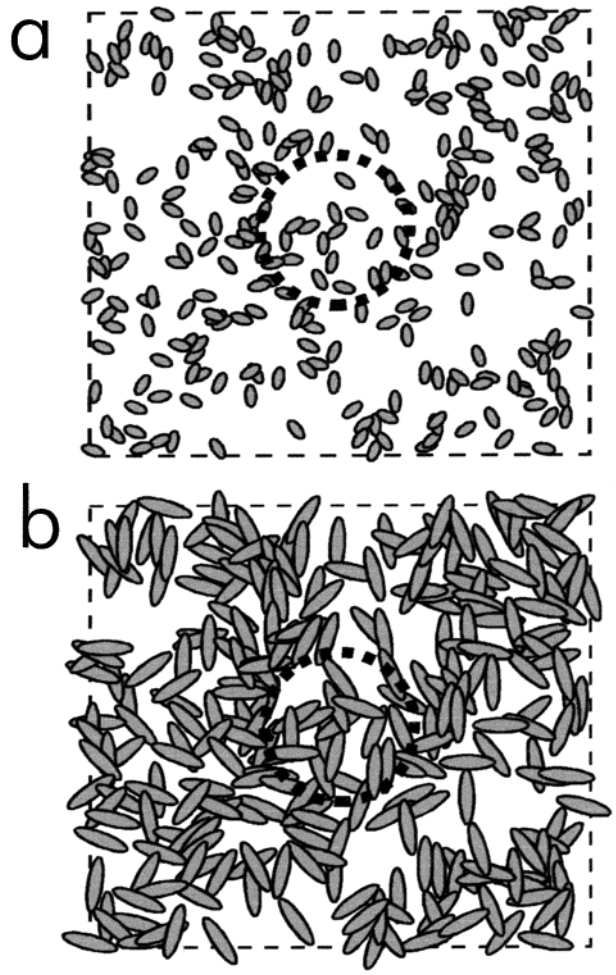

Figure 1. Simulated bilayer planes with side of 20 μm according to the model of Coelho et al.[14] for two rigid to fluid fractions: (a) 0.20 and (b) 0.47 (the percolation threshold for this system). For the purpose of comparison, we also represent the dimension of the spot of the FRAP experiments as a circle centered in the square.

The fluorescence recovery curves obtained were used by Coelho et al.[14] to draw conclusions indirectly about the geometry and topology of the separated phases in the two component lipid bilayers. By simulating the time regime of the experimentally observed FRAP data for the system dimyristoyl-*sn*-glycero-3-phosphocholine/distearoyl-*sn*-glycero-3-phosphocholine (DMPC/DSPC) 50/50 [10] with Monte Carlo techniques, they were able to predict possible shapes and dimensions of domains that could result in the obtained recoveries. In the analysis, they used two different topological models: the "fixed-ellipse model" consisting of identical solid ellipses increasing in number with the increase of the rigid fraction, and the "growing-ellipse model" in which a fixed number of ellipses grow in size until they fill the fraction of area occupied by the rigid phase. Both described quite adequately the experimental data from pure fluid, to fluid fractions below, but near, the percolation threshold of the system. This suggested that both models estimated with in a reasonable approximation the geometrical characteristics of the fluid domains relative to the radius of the FRAP spot until a relatively high rigid fraction was reached. Whatever the model used, for fluid fractions around 0.4, near the percolation threshold, ellipses with a major semiaxis, a, of 1.0 μm and aspect ratio b/a equal to 0.3 were predicted.[14] In Figure 1, we picture the topology of a bilayer of DMPC/DSPC 50/50 with fractions of fluid of 0.20 and of 0.47 according to the "growing-ellipse model".

It remains unclear why these domains are so much smaller than those observed in monolayers. Obviously, it should result from the interaction between domains in two opposed monolayers since it has been experimentally proved by Almeida et al.[9] that, at least in the case of DMPC/DSPC mixtures, the rigid domains are symmetric with respect to the bilayer central plane. Conversely, for mixtures of the nonzwitterionic *N*-lignoceroyldihydrogalactosylceramide with DPPC (a zwitterionic lipid), the same authors showed that the solid domains are not superimposed across the lipid bilayer. Because the rigid domains are richer in the component with higher transition temperature, the ceramide, the dipole density in the rigid domains can be similar or smaller than that of the fluid matrix. However, a quantitative reasoning is impossible because we do not know the dimension of the domains formed.

Some years ago, Keller et al.[15,16] presented a model with which they were able to rationalize the physics of the dispersion and the elongated shape of the rigid domains in phase separated monolayers of mixed lipids.

In this work, we develop a model for phase separated fluid bilayers based on the same reasoning of Keller et al. for the case of monolayers, but now adding the interactions between the two opposed rigid domains present in a bilayer. With this formalism, we are able to explain the much smaller dimension observed, and we also find that a circular-to-elliptic transition is to be expected, a transition that is in every aspect similar to what has been predicted for monolayers.[16]

Model and Basic Equations

In a bilayer, the excess energy of an uncharged polarized domain, E_b, here conceived as a rigid domain spanning across the bilayer, is the sum of the electrostatic energy of each monolayer domain, E_m, with the energy of the interface between the rigid and fluid bilayer regions, E_p, and the energy of interaction between the two monolayer domains, E_{int}

$$E_b = 2E_m + E_p + E_{int} \tag{1}$$

In calculating a variable part of the electrostatic energy related with a phase transition, we need consider only the difference in dipole density between fluid (μ_f) and solid (μ_g) phases. Therefore, we may regard the system as if there were no dipole in the fluid matrix and as if the dipole density (polarization) in the rigid domain were $\mu(\equiv \Delta\mu = \mu_g - \mu_f)$. In our case, E_m will be calculated as the energy resulting only from the vertical polarization of each monolayer domain considered as a plate with uniform vertical polarization. The monopole contribution due to the net charge at the interface will not be considered because our bilayers are zwitterionic and the aqueous media is considered to be of moderate ionic strength (in the referred work a 10 mM sodium phosphate buffer with added 50 mM potassium chloride was used). According to Keller et al.,[16] for uncharged polarized ellipses with principal radii a and b, thickness t, and vertically oriented molecular dipoles, at a distance d from each other resulting in a dipole moment per unit area μ, the electrostatic energy of a single monolayer is

$$E_m = \frac{1}{\epsilon_m}\left[\frac{2\pi A}{t}\mu^2 + \mu^2 R\int_0^{2\pi}\left(\psi \ln\frac{d}{4R\psi} + \frac{2\cosh\Delta}{\psi}\right)d\bar{\phi}\right] \tag{2}$$

where $\psi = \sqrt{\cosh\Delta + \sinh\Delta\cos 2\bar{\phi}}$, $\Delta = \ln(b/a)$ the logarithm of the aspect ratio of the ellipse, $R = \sqrt{ab}$, A is the area of the ellipse, and ϵ_m is the mean relative dielectric permittivity in the plane of the monolayer dipole system calculated as the average

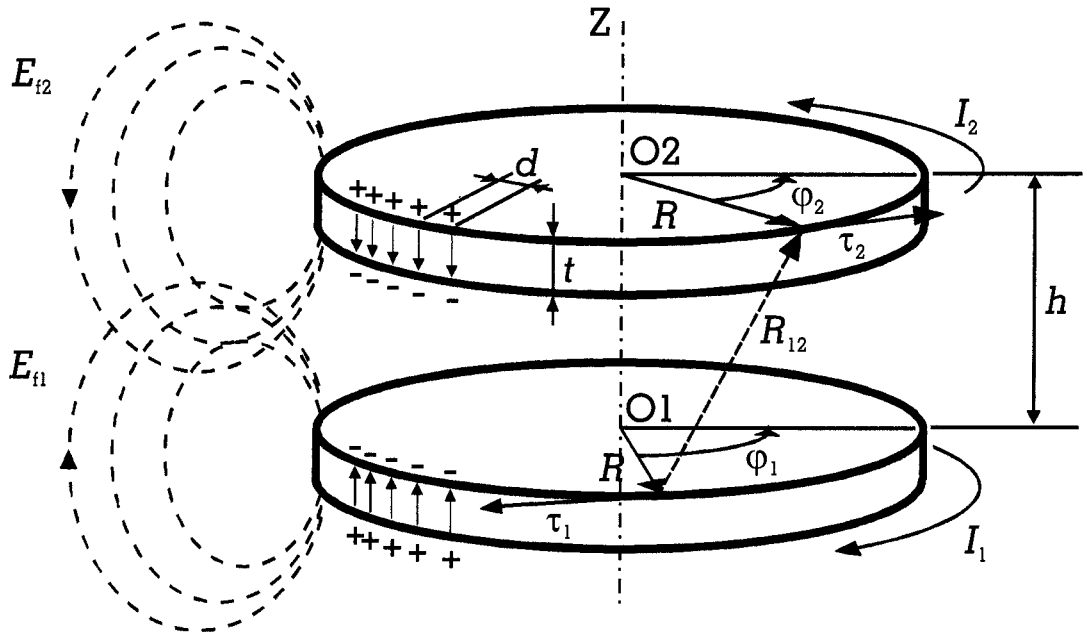

Figure 2. Diagram representing the two polarized surfaces of a rigid circular domain of radius R from a bilayer with thickness h, being t the thickness of each polar layer. The polar characteristics of these disks are conferred by vertically oriented molecular dipoles, μ_{mol}, at a distance d from each other. Also shown are the currents I_1 and I_2 that produce the fringe electrical fields E_{f1} and E_{f2} equivalent to those arising from the polar characteristics of each surface.

between that of the water in the vicinity of the headgroups, ϵ_{ext}, and that of the hydrocarbon region, ϵ_{int}. Because we want to evaluate the excess energy of the rigid domain relative to the surrounding fluid, μ stands for $\Delta\mu$, the difference between the dipole density in rigid and fluid regions of the same bilayer.

In Figure 2 the geometry of the pair of monolayer domains is presented.

The energy term E_p due to the interfacial line tension between rigid and liquid crystalline phases of the bilayer domain is given by

$$E_p = \lambda_b P \tag{3}$$

where λ_b is the interfacial line tension of the bilayer that, in the absence of a better approach, we will consider as being twice the line tension for the monolayer, λ_m, and P the perimeter of the domain.

Let us now estimate E_{int}, the interaction energy of the two apposed monolayer domains represented in Figure 2. As it follows from Maxwell's electrodynamic equations, the fringe field created by the uniformly distributed vertical electrical dipoles of each monolayer domain is physically equivalent to the magnetic field originated from a circular current loop.[16] Hence, the contribution to the energy of the bilayer domain coming from the interaction between these two dipole systems is equivalent to that of two interacting circular conductors, and is given by eq 4

$$E_{int} = -\frac{I_1 I_2}{\epsilon_{int} c^2} L_{12} \tag{4}$$

where the induction coefficient of the two fringe fields created by each of the monolayers is

$$L_{12} = \oint_{L_1}\oint_{L_2} \frac{d\vec{\tau}_1 d\vec{\tau}_2}{\vec{R}_{12}} \tag{5}$$

and the circular currents, I_1 and I_2, that would generate an equivalent fringe field are given by $|\vec{I}_1| = |\vec{I}_2| = |\mu\ c|$, $\vec{I}_i = |\vec{I}_i|\vec{\tau}_i$, where $\vec{\tau}_i$ is the unit tangential vector collinear with the current. The polarization density, μ, created by the vertical dipole moments was already defined, c is the speed of the light in the vacuum, and L_i the contours of each monolayer sub-system.

Equation 4 may also be written as

$$E_{int} = \frac{4\pi\mu^2 R}{\epsilon_{int}} F \tag{6}$$

where F is the modulus of the repulsive force between rigid domains resulting from polarization. This force is not simple to obtain from direct solution of eq 5 because the integral in this equation does not have analytical solution for an elliptical geometry. However, we have succeeded in obtaining a numerical solution of eq 5 as a function of Δ and $\xi = h/R\sqrt{\pi}$.

The value of $F(\Delta, \xi)$ calculated by numerical solution of eq 5 can be approximated by a polynomial in Δ and ξ which is very convenient for the calculation of E_{int} with eq 6. Because of later requirements of the calculation process it is advantageous to express F in terms of even powers of Δ with coefficients that are functions of ξ

$$F \cong F_0 + F_2\Delta^2 + F_4\Delta^4 \tag{7}$$

where

$$F_0 \cong -1.005 \ln \xi + 0.057 + 0.177\,\xi + 0.160\,\xi^2$$

$$F_2 \cong -0.064 \ln \xi + 0.004\xi^2 \tag{8}$$

$$F_4 \cong -0.003 \ln \xi - 0.001\xi^2$$

Equations 7 and 8 are an excellent approximation of F (deviations are smaller than 3%) for $h/R < 1$, being adequate to calculate E_{int}.

In Figure 3a, the variation of F with Δ, calculated for several values of ξ, is presented. It is interesting to observe that,

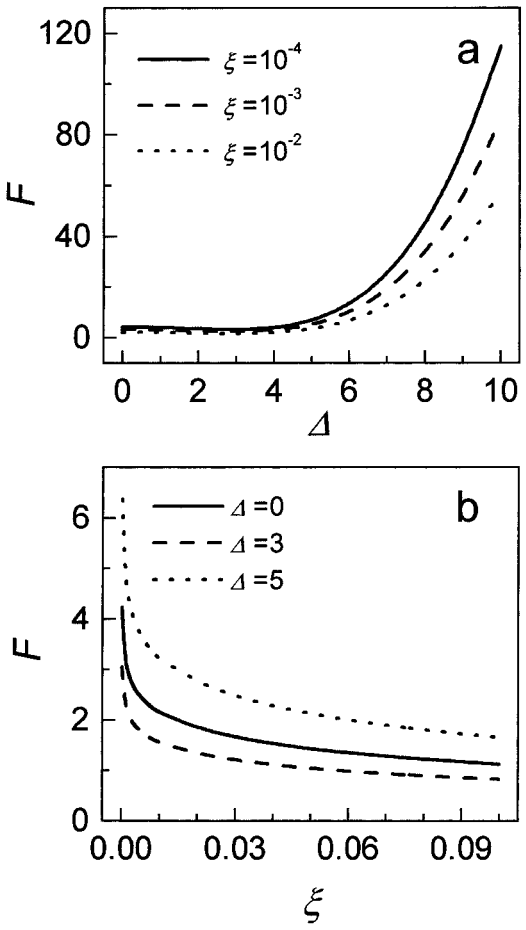

Figure 3. Repulsion force of two apposed rigid domains calculated with equations (7) and (8). In (a) variation with Δ for different $\xi = h/R\sqrt{\pi}$, and in (b) the variation with ξ for several Δ.

although for circular domains, $\Delta = 0$, the repulsion force is very small, for needlelike domains it becomes very large. Also, as could be anticipated, for the same aspect ratio a monotonic decrease of F with h/R for constant R is predicted by this equation as depicted in Figure 3b. However, in this figure it is evident that the curve for $\Delta = 3$ is lower than those for $\Delta = 0$ and 5 due to the fact that, irrespective of the value of ξ, the repulsive force between polarized domains has a minimum around $\Delta = 3$ ($b/a = 20$) which is not apparent in Figure 3a due to the scale used.

With the presented formalism, eqs 2, 3, and 6, we are able to analyze the complete energetics of a pair of apposed monolayer domains in a bilayer as a function of their geometry, R and b/a, and also as a function of the bilayer intrinsic properties, ϵ_{int} and h, using eq 1. In this way, the relative stability of large domains as compared to smaller ones and the possibility of transitions between a circular and an elliptic shape can be evaluated.

Circular to Elliptic Phase Transition

Following the methodology used by Keller et al.,[15,16] we will expand the expression for the energy of the elliptic bilayer domain into Taylor's series (using dimensionless variables)

$$\tilde{E}_b = \frac{E_b \epsilon_m}{4\pi\mu^2 h} = A\,y + B\,y\Delta^2 + C\,y\Delta^4 + ... \qquad (9)$$

where

$$A = \frac{\pi h}{t}\,y - \ln\left[\frac{\zeta y}{e^{2+\alpha}}\,e^{-\beta F_0}\right]$$

$$B = \frac{3}{16}\,\frac{\zeta y}{e^{10/3+\alpha}}\,e^{-16/3\beta F_2}$$

$$B = -2^{-10}\ln\left[\frac{\zeta y}{e^{46/3+\alpha}}\,e^{-2^{10}\beta F_4}\right]$$

with $\alpha = \epsilon_{ext}\,\lambda_b/\mu^2$, $\beta = \epsilon_{ext}/\epsilon_{int}$, $\zeta = 4h/d$, and $y = 1/\xi = R\sqrt{\pi}/h$.

Now all needed information concerning the stability of the elliptic vs circular geometry may be obtained from an analysis of the excess energy presented in eq 9.

The boundary condition for the rigid domain being at equilibrium relative to its shape is

$$\frac{d\tilde{E}_b}{d\Delta}\Big|_{\Delta^*} = 0 \qquad (10)$$

and it will correspond to a minimum of E_b when

$$\frac{d^2\tilde{E}_b}{d\Delta^2}\Big|_{\Delta^*} > 0 \qquad (11)$$

where the asterisk stands for equilibrium.

For the polarized uncharged ellipse the minimization of the energy gives two roots

$$\Delta^* = 0$$

$$\Delta^* = \pm\left\{\frac{96\ln(y/y_{cb})}{12 - \ln(y/y_{cb}) + \beta\left[2^{10}F_4(y) - \frac{16}{3}F_2(y_{cb})\right]}\right\}^{1/2} \qquad (12)$$

$$\cong \pm\left(\frac{96\ln\tau}{p + q\ln\tau}\right)^{1/2}$$

where $\tau = y/y_{cb}$, $y_{cb} = R_{cb}\,\pi/h$, $p \cong 12 + 3.413\,\beta\ln y_{cb}$, and $q \cong 3.072\beta - 1$, and the subscript cb means that the parameter has the critical value for the shape transition in the case of the bilayer.

The variation of R_{cb} with α, depicted for $h = 4.0$ nm and $d = 0.8$ nm in Figure 4a, shows that an increase in the line tension for constant μ and ϵ_{ext} (increase in α) results in an increase in R_{cb} due to the larger perimeter of an ellipse when compared with the circle with identical area, and the effect is more pronounced for large dielectric permittivity of the core of the bilayer resulting in a larger interlayer interaction. In the same way, a larger R_{cb} is obtained for smaller interaction intra- and inter monolayers due to a smaller dipole density or higher external permittivity, resulting in a larger α value. In the case of a typical bilayer, e.g., a bilayer of dipalmitoyl-*sn*-glycero-3-phosphocholine, DPPC, $\lambda_p = 1.6 \times 10^{-6}$ erg cm^{-1}, $\mu = 2 \times 10^{-3}$ statvolt cm/cm^2, and taking $t = 0.4$ nm,[17] if $\epsilon_{ext} = 30$ and $\epsilon_{int} = 3$ ($\beta = 10$) the transition will take place when the domains are still very small $R_{cb} > 50$ nm. If we consider that the permittivity of the external medium is near 80, then, the transition will occur for much larger domains with R_{cb} of ca. 1 μm. It is also interesting to see how the critical radius for the circular to elliptic geometry transition changes with the thickness of the bilayer, h. In Figure 4b it is shown that a destabilization of the circular shape for thinner bilayers is to be expected.

When $\tau \to \infty$, that is for $R \gg R_{cb}$, we obtain for $\beta = 20$ $\Delta^* \to \pm 1.125$ equivalent to $a/b \cong \{^{0.32}_{3.02}$ that is an ellipse with

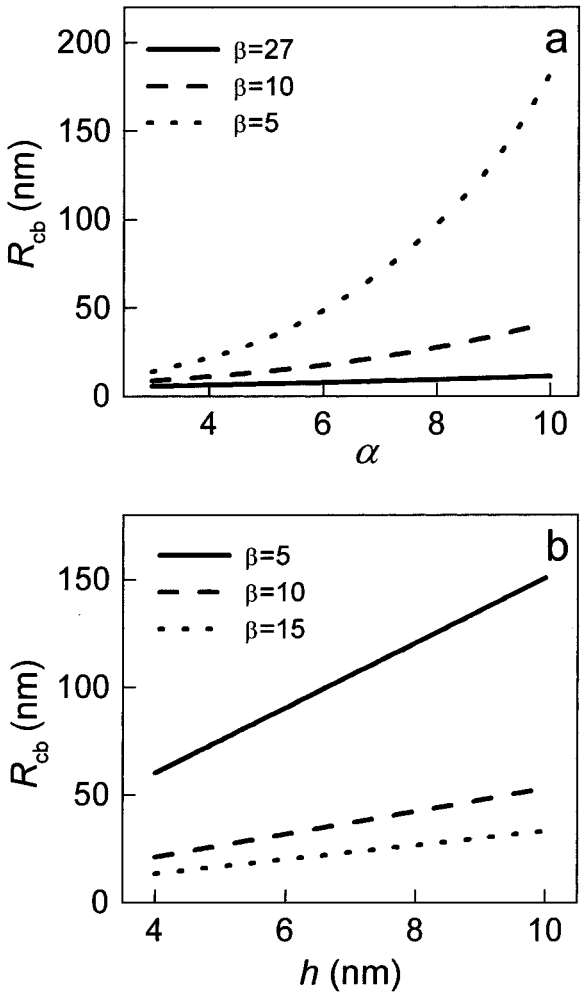

Figure 4. Critical mean radius of circular to elliptic shape transition for the bilayer, R_{cb}, as a function of $\alpha = \epsilon_{ext}\lambda_b/\mu^2$ for several values of β (a), and as a function of h for different values of the dielectric permittivity ratio, β, (b).

aspect ratio 0.32 in coincidence with the value of 0.3 advanced by us for the aspect ratio of the ellipses obtained from the analysis of FRAP data with the fixed ellipse (ad hoc) parameters.[14] The fact of this agreement may be treated both as a justification of the FRAP data with their Monte Carlo simulation and a verification of our model and an approach.

A real root for the second equation in eq 12 exists only when $y \geq y_c$. The value $y = y_{cb}$ corresponds to the beginning of the shape transition and satisfies the equation

$$\frac{\zeta y_{cb}}{e^{10/3+\alpha}} e^{16\beta F_2/3} \tag{13}$$

Taking into account that $(1/\zeta)e^{10/3+\alpha}$ is the critical radius corresponding to the beginning of the shape transition in the equivalent monolayer domains[16] we can write

$$\frac{R_{cb}}{R_{cm}} = \frac{y_{cb}}{y_{cm}} = \exp\left[\frac{16}{3}\beta F_2(y = y_{cb})\right] \tag{14}$$

Allowing $h/R\sqrt{\pi} \ll 1$, a reasonable assumption for the bilayer, then

$$y_{cb} \cong y_{cm}^{(1+0.341\beta)^{-1}} = \left(\frac{1}{\zeta} e^{10/3+\alpha}\right)^{(1+0.341\beta)^{-1}} \tag{15}$$

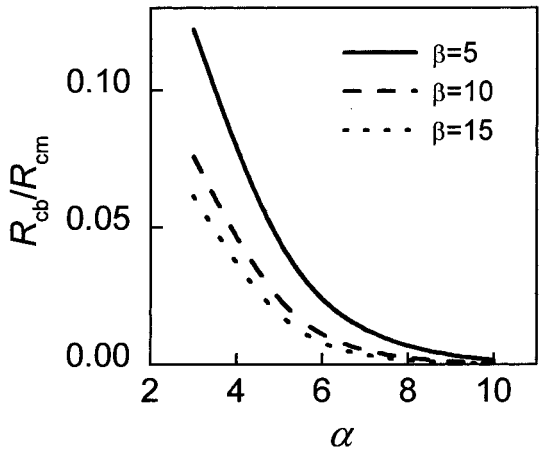

Figure 5. Variation of R_{cb}/R_{cm} with $\alpha = \epsilon_{ext}\lambda_b/\mu^2$ for $\beta = 5$, 10, and 15 the other parameters having the values typical of a DPPC membrane given in the text.

in this way

$$\frac{R_{cb}}{R_{cm}} = \frac{y_{cb}}{y_{cm}} \cong y_{cm}^{0.341\beta/(1+0.341\beta)} \ll 1, \text{ if } \beta \gg 1 \tag{16}$$

Therefore, $y_{cb} \ll y_{cb}$ and consequently, this transition which is believed to take place for submicroscopic domains in zwitterionic monolayers[16] is not, in principle, experimentally detectable in bilayers.

In Figure 5, we can compare the circle/ellipse transition in a bilayer and in a monolayer, R_{cb}/R_{cm}, as a function of α for a given bilayer core thickness, $h = 4$ nm, and different values of β. The increase of λ_b and/or decrease of μ give rise to an increase in α, which affects more the bilayer than the monolayer, as it would be expected.

Maximum Domain Size

Let us show that each large domain having reached some critical size, R_f, will be disintegrated in two smaller pieces, or, by other words, there is a maximal size of the domain, in accordance with experimental data. The evidence is based on pure thermodynamic considerations (without regarding the activation energy of the process), where from follows that the domains with radii larger R_f have bigger energies than a sum of their pieces. That is, if E_0 is the energy of an elliptic domain of radius R and area S_0, and this domain breaks in two smaller ones with energy E_1 and E_2 and areas S_1 and S_2 such that $S_0 = S_1 + S_2$, there will be a critical radius of fission of the large elliptic domain, $R = R_{fb}$, above which $E_1 + E_2 < E_0$.

It may be easily demonstrated that the energy of the resultant domains is minimal when two circles with identical radius are formed. Thus, we consider the fission of a large elliptic domain in two circular ones with equal area. In this way, the critical radius for fission of a bilayer domain, R_{fb} has to verify the equation $E_0(R_{fb}) = 2E(R_{fb}/\sqrt{2})$, where E is the energy of the circular domain with radius $R_{fb}/\sqrt{2}$. Using eq 9 the energy condition may be rewritten as eq 17 where $y_{fb} = R_{fb}/\sqrt{\pi}/h$ is the critical parameter of fission for a given membrane height.

$$A(y_{fb}) + B(y_{fb})\,\Delta^2(y_{fb}) + C(y_{fb})\,\Delta^4(y_{fb}) = \sqrt{2}\,A(y_{fb}/\sqrt{2}) \tag{17}$$

Withholding only the terms of lower orders, after some algebraic

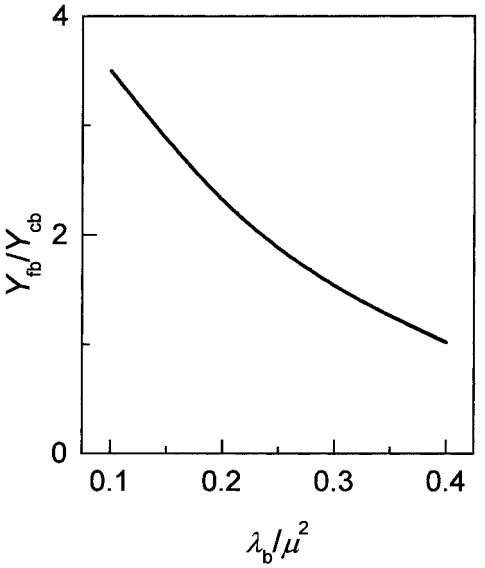

Figure 6. Comparison of the mean radius for fission with that for shape transition for a DPPC lipid matrix as a function of λ_b/μ^2. For this plot, we have used $\epsilon_{ext} = 25$.

manipulation this formula is reduced to a cubic equation

$$x^3 + Px^2 + Qx + R = 0 \qquad (18)$$

Here, $x = \ln(y_{fb}/y_{cb})$ is a variable that measures the fission geometry in terms of the circle to elliptic spontaneous transition; the coefficients P, Q, and R in this equation depend only on the dimensionless parameters $\beta = \epsilon_{ext}/\epsilon_{int}$ and $y_{cb} = R_{cb}\sqrt{\pi}/h$, and the subscripts c and b refer respectively to the critical value for circle to ellipse transition of the bilayer domain. In this way, we establish a relation between R_{fb} and R_{cb} that allow the evaluation of the variation of the maximum domain size for any given parameters of the system.

One should note that if in eq 18 we make $\beta = 0$ (thereby "switching off" the dipole interaction between two dipole domains at the bilayer interfaces), we are in the case of a monolayer domain where no interaction between layers occur. In this case, for the already given values of y_{cb} (and therefore constants P, Q, and R), the eq 18 has only one real root, $x_m^* \cong 0.28$, where x_m refers to the monolayer, therefore being $y_{fm} \cong 1.32\, y_{cm}$. This result clarifies the apparent paradox obtained by other authors[16] for the fission of a circular monolayer domain in two smaller ones. The reason for their result, $y_{fm} < y_{cm}$, may be due to them having not considered the intermediacy of an elliptic shape in the fission process as we do.

Let us consider the consequences of the cubic eq 18 for the maximal dimension of the domains in a bilayer. In Figure 6, the variation of y_{fb}/y_{cb} ($=R_{fb}/R_{cb}$) is presented as a function of λ/μ^2 for the same parameters used in the previous plots and $\epsilon_{ext} = 25$. For low values of λ/μ^2, the fission takes place for $y_{fb} > y_{cb}$, that is, the domains are already elliptical when they attain their maximum stable area.

Using the already given values for the parameters d, λ_p, and μ characteristic of a DPPC bilayer, and for values of the external dielectric permittivity ranging from 30 to 80, which are those found in the literature for the medium in the immediate vicinity of the bilayer interface, we have plotted in Figure 7a and b the dependence of R_{fb} respectively, on h and ϵ_{int}. Maintaining constant all the other parameters, plots in Figure 7a, made for $\epsilon_{int} = 3$, show a very small dependence of R_{fb} on the bilayer core thickness, h. Contrasting with this behavior, R_{fb} increases

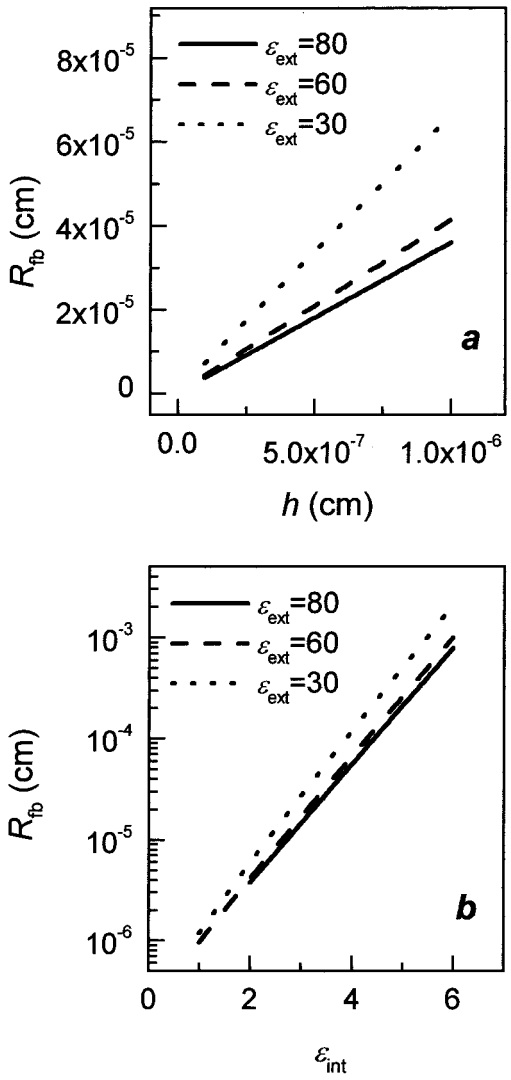

Figure 7. Plot of the fission radius of the bilayer domains, R_{fb}, as a function of the thickness of the hydrophobic region for $\epsilon_{int} = 3$, panel **a**, and of the internal dielectric permittivity for $h = 4.0$ nm, panel **b**. All the remaining parameters as given in the text.

sharply with increasing of the internal dielectric permittivity of the core of the membrane, resulting from the decrease in the density of the interacting electric field, as shown in Figure 7b for $h = 4.0$ nm. It is worth to note that this effect is relatively insensitive to ϵ_{ext} (comparing with the effect of ϵ_{int}). The fact that the fission radius of the bilayer domain is much smaller than that for monolayers comes to meet what we want to prove. It is, however, remarkable, that the theoretical estimations of the maximal domain dimensions, ranging from 0.1 to1.0 μm (for ϵ_{int} between 3 and 4) are in so good agreement with the experimental results.[14]

Conclusions

The data in Figure 7 shows that there are electrostatic reasons for the fission of a bilayer domain to take place for geometric dimensions much smaller than those observed for monolayers with identical composition. Taking into account the imperfections of the model used, the value for the fission radius has not much meaning in itself despite the fact that it agrees with the number expected.

The agreement between the theoretical calculations and the FRAP data joint with the Monte Carlo simulation (namely, the

maximal domain size, $R_f \approx 0.1-1.0$ μm, and the ellipse axis relationship, $a/b \approx 0.3$) has verified both the "ad hoc" assumptions in the Monte Carlo model simulation[14] and the adequacy of the proposed approach, despite the fact that we did not took into account the interaction between the in-plane components of the dipoles and the monopole contribution.

The weak dependence of R_{fb} on the thickness of the membrane, especially for the higher values of ϵ_{ext}, does not allow us to test the validity of the model by using lipids of different chain lengths, this because the thickness of a bilayer cannot be widely changed. However, we are presently working on the possibility of using the strong dependence of R_{fb} on the dielectric permittivity of the bilayer core to experimentally test our model.

Also interesting is the conclusion that, similarly to what was predicted for monolayers, there is a shape transition from a circular to elliptic geometry in bilayers taking place in the early stages of domain formation. This transition has, to our knowledge, never been unequivocally observed in monolayers and its physical meaning for the case of bilayers is questionable. In fact, a domain with $R = 10$ nm, see Figure 4, contains ca. 750 phospholipid molecules and it is more reasonable to be considered a perturbation than a separated phase.

Acknowledgment. This work was supported in part by the program PRAXIS from the Fundação para a Ciência e Tecnologia, Portugal. V.S. is indebted to PRAXIS−Portugal for the grant bcc/4346/94.

References and Notes

(1) Marsh, D. *CRC Handbook of Lipid Bilayers*; CRC Press: Boca Raton, FL., 1990; p 234.

(2) Lösche, M.; Sackmann, E.; Möhowald, H. *Ber. Bunsen-Ges. Phys. Chem.* **1983**, *87*, 848.

(3) Peters, R.; Beck, K. *Proc. Natl. Acad. Sci. U.S.A.* **1983**, *80*, 7183.

(4) Weis, R. M.; McConnell, H. M. *J. Phys. Chem.* **1985**, *89*, 4453.

(5) Hwang, J.; Tamm, L. K.; Böhm, C.; Ramalingam, T. S.; Betzig, E.; Edidin, M. *Science* **1995**, *270*, 610.

(6) Hwang, J.; Gheber, L. A.; Margolis, L.; Edidin, M. *Biophys. J.* **1998**, *74*, 2184.

(7) Korlach, J.; Schwille, P.; Webb, W. W.; Feigenson, G. W. *Biophys. J.* **1999**, *96*, 8461.

(8) Bagatolli, L. A.; Gratton, E. *Biophys. J.* **2000**, *78*, 290.

(9) Almeida, P. F. F.; Vaz, W. L. C.; Thompson, T. E. *Biochemistry* **1992**, *31*, 7198.

(10) Vaz, W. L. C.; Melo, E. C. C.; Thompson, T. E. *Biophys. J.* **1989**, *56*, 869.

(11) Vaz, W. L. C.; Melo, E. C. C.; Thompson, T. E. *Biophys. J.* **1990**, *58*, 273.

(12) Bultmann, T.; Vaz, W. L. C.; Melo, E. C. C.; Sisk, R. B.; Thompson, T. E. *Biochemistry* **1991,** *30*, 5573.

(13) Almeida, P. F. F.; Vaz, W. L. C.; Thompson, T. E. *Biophys. J.* **1993**, *64*, 399.

(14) Coelho, F. P.; Vaz, W. L. C.; Melo, E. *Biophys. J.* **1997**, *72*, 1501.

(15) Keller, D. J.; McConnell, H. M.; Moy, V. T. *J. Phys. Chem.* **1986**, *90*, 0, 2311.

(16) Keller, D. J.; Korb, J. P.; McConnell, H. M. *J. Phys. Chem.* **1987**, *91*, 6417.

(17) Benvegnu, D. J.; McConnell, H. M. *J. Phys. Chem.* **1992**, *96*, 6820.